Flow compensation in a MEMS dual-thermal conductivity detector for hydrogen sensing in natural gas

de Graaf, G; Abarca Prouza, Accel; Wolffenbuttel, RF

DOI
10.1109/TRANSDUCERS.2015.7181145

Publication date
2015

Document Version
Accepted author manuscript

Published in
Proceedings of the 2015 Transducers - 2015 18th Solid-State Sensors, Actuators and Microsystems, TRANSDUCERS 2015

FLOW COMPENSATION IN A MEMS DUAL-THERMAL CONDUCTIVITY DETECTOR FOR HYDROGEN SENSING IN NATURAL GAS

G. de Graaf[1], *A. Abarca Prouza*[1], *and R.F. Wolffenbuttel*[1]
[1]Delft University of Technology, The Netherlands

ABSTRACT

Conventional thermal conductivity detectors (TCDs) demonstrate a flow dependence. The approach presented here to reduce the flow dependence is based on the on-line flow compensation using two thin-film sensors on membranes in parallel on the same chip that are differentially operated. These are laterally identically, but with a different depth of the detection chamber, resulting in different quasi-static sensitivities to the thermal conductivity of the sample gas. The effects of conduction and convection in the structure have been studied using COMSOL Multiphysics. First prototypes have been fabricated and are presently tested.

KEYWORDS

Thermal conductivity detector, flow compensation, Hydrogen sensor, MEMS.

INTRODUCTION

Gas sensors are increasingly used in the growing markets of automotive industry and environmental monitoring [1]. The most common gas sensors are based on chemical interaction [2]. These sensors measure a change in the conductance or other physical property between the gas and the sensing material during gas interaction [3]. These sensors have a high sensitivity [4]. However, they are not reliable in long-term use, because of chemical contamination of the sensing part [3, 5].

On the other hand, the use of gas sensors based on thermal conductivity detection has increased due to advances in the area of integrated circuit (IC) technology [6]. TCDs are widely utilized in control process and especially in gas chromatography (GC) [7, 8]. TCDs are very suitable to detect hydrogen, because the thermal conductivity of hydrogen is around 7 times higher than that of air. The main advantage as compared to chemical sensors is that the operation of a TCD is not affected by chemical contamination in long-term use, making it very reliable and robust. In addition, MEMS technology enables miniaturization at low cost [6].

A TCD measures the thermal conductivity of a gas by means of a heated element in the gas stream. The heat loss through the gas is measured. The most common TCDs are the so called hot-wire devices [7]. Basically, the hot-wire acts as a heater and temperature sensor at the same time. An electric current through the wire produces Joule heating and, depending on the surrounding gas, the temperature of the wire changes and can be detected as a change in resistance. Another approach is to separate the hot element and the temperature sensor using MEMS processing technology, making the design more flexible [9].

One of the major issues of this type of sensors is their flow dependence. It is necessary to calibrate the sensor depending on the flow rate for every gas in the gas stream. Moreover, the flow affects the measured temperature. A flow independent design could avoid the re-calibration for each gas. An approach of a flow independent TCD has been proposed by [10] based on the division of the TCD in several independent TCD sections, whereby the gas is pre-heated in the first region, thus making the actual measurement less dependent on the flow.

A flow-independent dual-TCD is proposed in this work and will be explained in the following section.

DESCRIPTION OF THE DEVICE

The proposed dual-TCD is composed of two identical devices fabricated on the same substrate, as shown in Fig. 1. Each device consists of a heating element, in this case a resistor, and thermopiles acting as temperature sensors placed to each side of the heater. Both structures are fabricated on top of a thin membrane. Underneath each heater there is a detection chamber which is filled with the gas. Holes or slits in the membrane enable transport of the gas into the chamber at a flow rate as can be seen in Fig. 1(a). One of the chambers is very shallow having a depth of 2 μm while the other chamber is considerably deeper, having a full-wafer depth of 525 μm (Fig. 1(b)).

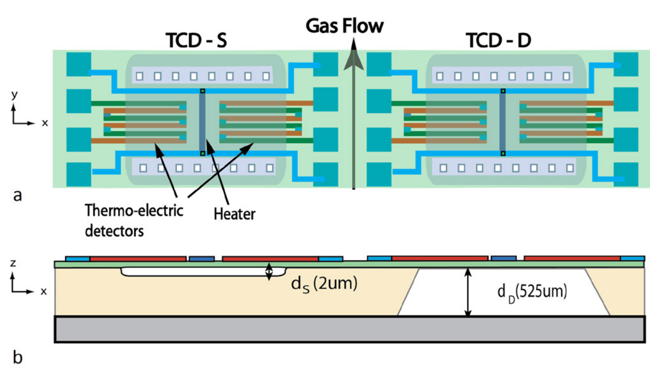

Figure 1: Dual-TCD device. (a) Top view of the device. (b) Cross section of the dual-TCD.

Description of the Method

Both heaters are fed by a current source producing heat by Joule heating effect. The heat spreads over the thin membrane where the thermopiles measure the temperature difference between the heater and the substrate. The membrane temperature, as measured by the thermopiles, is kept constant at a certain value above ambient by controlling the current supply of the heaters. The heat loss of the shallow cavity (SC) device and the depth cavity (DC) device is given by the total thermal conductance G which is proportional to the total power of each device. The total power is given by:

$$P = \Delta T \cdot G \tag{1}$$

where ΔT is the temperature difference between the heater and substrate (ambient). Neglecting radiation effects, G can be split as follows:

$$G = G_b + G_g + G_c \tag{2}$$

with G_b the thermal conductance of the beam, G_g the thermal conductance through the gas, and G_c corresponds to the heat loss by convection. Keeping both sensors at the same temperature and since the beam conductivity and the heat loss due to convection are identical, the terms G_c and G_b are equal and the power difference can be written as

$$\Delta P = P_S - P_D = \Delta T(G_{gS} - G_{gD}) \tag{3}$$

where G_{gS} corresponds to the SC device and G_{gD} corresponds to the DC device. The power difference depends on the difference in the thermal conductance in the sample chamber G_g of the SC device and the DC device. At the same time, the thermal conductance of the gas G_g can be approximated by:

$$G_g = \frac{\lambda_g A}{d} \tag{4}$$

where λ_g is the thermal conductivity of the gas, A is the area of the membrane and d is the depth of the cavity. Substituting Eq. (4) in (3) results in the power difference, which is expressed as:

$$\Delta P = \Delta T\left(\frac{\lambda_g A}{d_S} - \frac{\lambda_g A}{d_D}\right) = \Delta T \lambda_g A\left(\frac{1}{d_S} - \frac{1}{d_D}\right) \tag{5}$$

Since the depth of the cavity d_D is much larger than d_S, the second term of Eq. (5) can be almost neglected. Operation at a constant temperature difference ΔT results in:

$$\Delta P \approx \Delta T \frac{\lambda_g A}{d_S} \tag{6}$$

Equation 6 shows that the power difference of both devices is proportional to the thermal conductivity of the gas, independent on the gas flow and the thermal conduction of the supporting structure. Substitution of some typical values of the presented structure show that the heat loss through the beam suspension is much lower than the heat loss by conduction through the gas inside of the chamber of the SC device making the sensor very sensitive to the thermal conductivity of the gas inside the shallow chamber.

DESIGN AND FABRICATION OF THE DUAL-TCD

Different versions of the sensor are being fabricated following the MEMS process presented in [9]. The sensor is fabricated on a 525 µm silicon wafer with a 4 µm layer of sacrificial silicon-dioxide. A layer of 600 nm of silicon nitride forms the basic membrane. The heating elements are patterned layers of 0.3 µm doped polysilicon. After this the structure is protected by a 0.3 µm of SiN. Finally free standing structures are formed by vapour HF etching of the sacrificial layer through etching holes. The top area of the device is 464 µm x 154 µm having a height of 526.2 µm. The etched and venting holes are 4 µm x 4 µm.

SIMULATIONS AND RESULTS

The dual-TCD is designed and simulated using COMSOL Multiphysics 4.4. Two kinds of simulations were performed: static and dynamic. Static simulations were made without a gas flow passing through the sensor and dynamic simulations were made using an input gas flow parallel to the heaters (Fig. 1(a)).

Static Simulations

The design of the sensor is shown in Fig. 2 using the dimensions stated in a previous section.

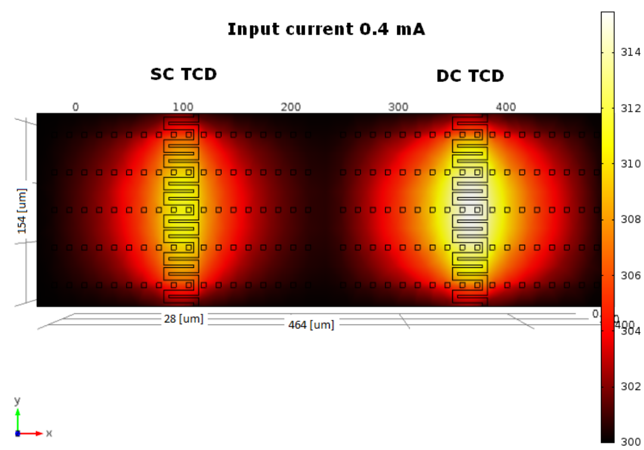

Figure 2: Dual-TCD device designed using COMSOL Multiphysics 4.4.

Figure 2 shows a temperature profile of the sensor. Feeding both heaters using an input current of 0.4 mA shows that the DC device reaches a higher temperature compared to the SC device due to the difference in the depth of the cavity. Thus, the DC TCD needs a smaller input current than the SC TCD to reach the same temperatures.

The simulations were made using the Physics module "Joule Heating" which combines electric and heat transfer behavior. To maintain a constant temperature of 310 K in the position of the thermopiles the input current densities in the polysilicon resistors were taken as a controlled parameter in the simulations. The total power of the devices is shown in Table 1 and the results have been plotted in Fig. 3.

Table 1: Static response of the dual-TCD: Required heater power for different gases for maintaining a constant temperature of the thermopile of 310 K.

Gas	Thermal conductivity λ [W/m·K]	SC TCD P [mW]	DC TCD P [mW]
Vacuum	0	5.29	5.29
CO_2	0.01622	7.81	5.38
N_2	0.02604	9.34	5.50
CH_4	0.03458	10.67	5.60
He	0.14200	25.71	6.89
H_2	0.18690	30.69	7.44

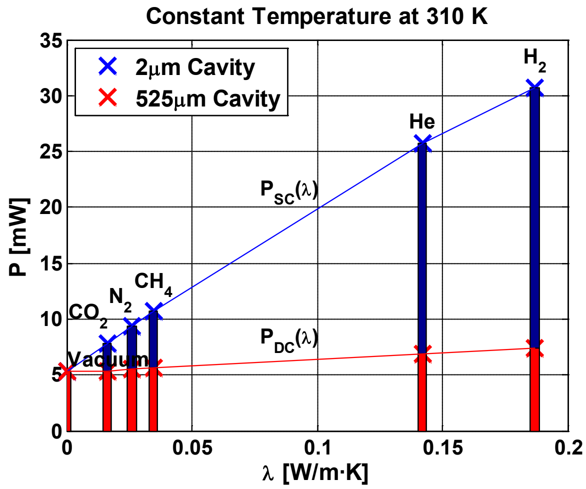

Figure 3: Heating power of both devices vs. thermal conductivity of the gases.

The simulations in vacuum show the effect of the conductivity of the suspension of the membranes (G_b). The results show that much more power is required to maintain a constant temperature in the SC TCD due to the large heat loss through the thin layer gas in the shallow cavity. As a result the SC TCD is much more sensitive to the gas thermal conductivity than the DC TCD which is basically just a compensation device. Fig. 3 shows that relation between the power dissipation and the gas thermal conductivity of both devices is almost linear:

$P_{SC}(\lambda) = 0.136 \cdot \lambda + 0.005$ [W] with a correlation coefficient $R^2 = 0.998$ and $P_{DC}(\lambda) = 0.012 \cdot \lambda + 0.005$ [W] with $R^2 = 0.998$. The sensitivity of the SC device is $S_\lambda = 0.136$ W/(W/m·K) while the sensitivity of the BC device is only $S_\lambda = 0.012$ W/(W/m·K).

Dynamic Simulations

These simulations were performed using the same model of Fig. 2 but in this case the physics module "Laminar flow" was added. Also, stationary and time dependent studies were simulated. Again the current density in the resistors has been used as a controlled variable to maintain a constant temperature of 310 K in the thermopiles for an input flow in the range between 1 to 10 ml/min. The values of the static simulations were used as a starting point.

The flow inside of the cavities was simulated and the results are shown in Fig. 4.

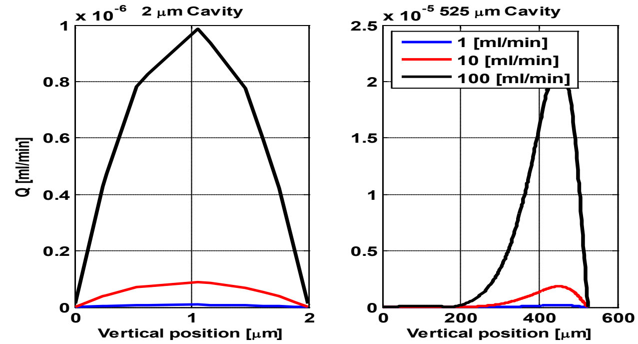

Figure 4: Flow profiles inside of the cavities.

Fig. 4 shows that the flow inside of the cavities is negligible which means that the heat loss inside of the cavities is mainly by conduction through the gas.

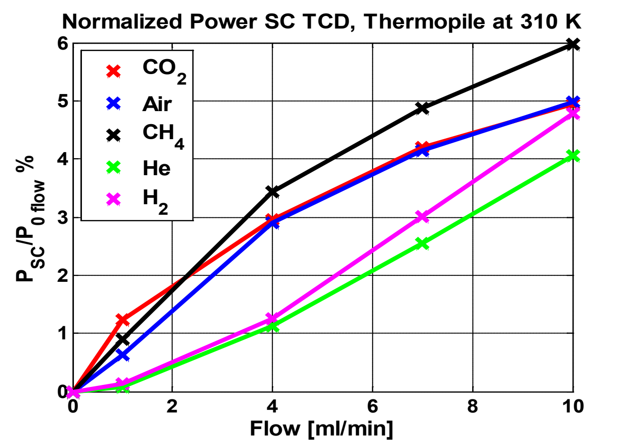

Figure 5: Relative change of the heating power of the SC device vs. flow for different gases.

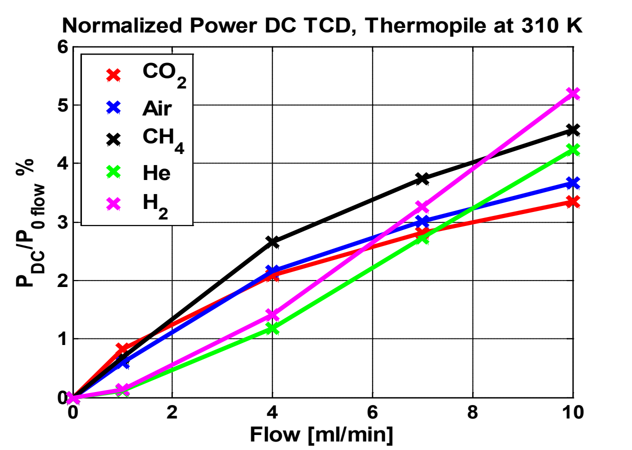

Figure 6: Relative change of the heating power of the DC device vs. flow for different gases.

Also, the time response of the sensor was calculated simulating the time required to fill both cavities resulting in a typical response time of t_G = 4 ms. The dependence of power signal to the flow rate for different gases for both devices is shown in Figures 5 and 6. Figures 5 and 6 clearly show the flow dependence of the devices requiring more power for large flows. The sensitivity of the SC device is S_F = 0.049 mW/(ml/min) and the sensitivity of the BC device is S_F = 0.040 mW/(ml/min).

The results of the power difference of both devices are shown in Table 2 and Fig. 7.

Table 2: Power difference for different flows and gases.

Gas	0 ml/min ΔP [mW]	1 ml/min ΔP [mW]	4 ml/min ΔP [mW]	7 ml/min ΔP [mW]	10 ml/min ΔP [mW]
CO_2	2.42	2.43	2.44	2.45	2.45
Air	3.79	3.79	3.82	3.83	3.84
CH_4	5.07	5.08	5.11	5.13	5.15
He	18.82	18.82	18.88	18.92	18.97
H_2	23.25	23.27	23.31	23.34	23.36

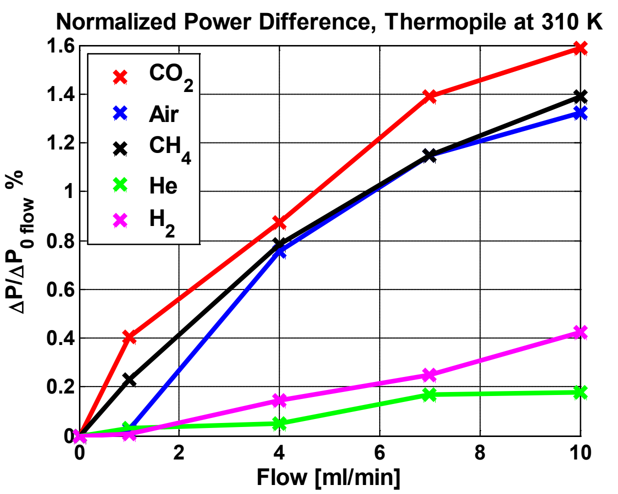

Figure 7: Power difference of the dual-TCD for different flows.

Table 2 and Fig. 7 show that ΔP remains almost constant for different flows, using different gases, confirming the concept of the flow independent Dual TCD principle.

CONCLUSIONS AND FUTURE WORK

The presented TCD has, due to the low thermal conductivity of the membrane suspension and the very thin layer of gas in the SC device, probably highest TCD sensitivity S_λ= 0.136 W/(W/m·K) available nowadays. The DC device has a significantly lower sensitivity S_λ= 0.012 W/(W/m·K). Simulations have shown that the flow inside of the cavities is limited to about 25 nl/min. This means that in the chamber the heat loss is mainly by conduction through the gas neglecting convective effects. The time response of the sensor was simulated resulting in t_G = 4 ms. Dynamic simulations also show that the heat loss caused by the flow above the membrane is not negligible. The SC and DC devices have identical flow sensitivity which enables flow compensation in differential operation at constant temperature. The power difference signal clearly shows a high sensitivity for the gas conductivity and a low flow dependency. Several versions of the Dual-TCD device are fabricated and will be characterized and tested at different flow rate to verify their sensitivity, the flow compensation principle and their long-term stability.

REFERENCES

[1] S. Ohira, and K. Toda, "Micro gas analyzers for environmental and medical applications", Abalytica Chimica Acta 619 (2008), pp. 143-156.

[2] L. Francioso, R. Rella, P. Siciliano, J. Spadavecchia, D. Presicce, A.M. Taurino, S. Capone, and A. _Forleo, "Solid state gas sensors: state of art and future activities", Journal of Optoelectronics and Advanced Materials, vol. 5, pp. 1335-1348, 2003.

[3] P. Tardy, J.-R. Coulon, C. Lucat, and F. Menil, "Dynamic thermal conductivity sensor for gas detection", Sensors and Actuators B, vol. 98, pp. 63-68, 2004.

[4] P.T. Moseley, "Solid state gas sensors", Meas. Sci. Technol., vol.8, No 3, pp. 223-237, 1997.

[5] S.J. Kim, "Gas sensors based on Paschen's law using carbon nanotubes as electron emitters", Journal of Physics D: Applied Physics, vol. 39, pp. 3026-3029, 2006.

[6] R.P. Manginell, J.H. Smith, and A.J. Ricco, "An overview of micromachined platforms for thermal sensing and gas detection", Proceedings of SPIE on International Society of Optical Engineering, pp. 273–284, 1997.

[7] H.A. Daynes, Gas Analysis by Measurement of Thermal Conductivity, Cambridge University Press, Cambridge, Great Britain, 1933, pp. 1–302.

[8] W. Jennings, E. Mittlefehldt and P. Stremple, Analytical Gas Chromatography, Second Edition, Elsevier Inc., ISBN-13: 978- 0-12-384357-9, 389 pages. Sep. 1997.

[9] G. de Graaf, and R.F. Wolffenbuttel, "Surface-micromachined thermal conductivity detectors for gas sensing", Instrumentation and Measurement Technology Conference (I2MTC), 2012 IEEE International, pp. 1861-1864, 2012.

[10] B. C. Kaanta, H. Chen and X. Zhang, "Novel device for calibration-free flow rate measurements in micro gas chromatographic systems", J. Micromech. Microeng. 20 (2010) 095034 (7pp) doi:10.1088/0960-1317/20/9/